PROBING QUANTUM GRAVITY THROUGH ASTROPHYSICAL OBSERVATIONS

By

STUART MARONGWE

Reg. No: 1610073

Lic.(Physics and Electronics) (Jose Varona, Cuba)

Department of Physics and Astronomy

Faculty of Science

Botswana International University of Science and Technology

stuart.marongwe@studentmail.biust.ac.bw, (+267)74001251

A Dissertation Submitted to the Faculty of Science in Partial Fulfilment of the Requirements for the Award of the Degree of Master of Science in Physics of BIUST

Supervisor: Dr. Mhlambululi Mafu

Department of Physics and Astronomy, BIUST

mafum@biust.ac.bw (+267) 4931567

Signature: Mhlambululi Mafu Date: 20/10/2020

March, 2020

DECLARATION AND COPYRIGHT

I, STUART MARONGWE, declare that this dissertation is my own original work and that it has not been presented and will not be presented to any other university for a similar or any other degree award.

Signature… 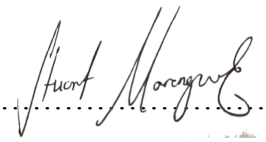 …… Date: 20/10/2020

CERTIFICATION

The undersigned certifies that he has read and hereby recommends for acceptance by the Faculty of Science a dissertation titled:

PROBING QUANTUM GRAVITY THROUGH ASTROPHYSICAL OBSERVATIONS, in fulfilment of the requirements for degree of masters of Science Physics of the BIUST.

Mhlambululi Mafu .....

Dr. Mhlambululi Mafu

(Supervisor)

Date: 20/10/2020

To Amadeus Cruz Marongwe

Contents

LIST OF TABLES

Abstract

This work is primarily focused on probing quantum gravity through astrophysical observations based on the theoretical framework of the Nexus Paradigm of quantum gravity. The Nexus Paradigm is a theoretical framework that is still in development and offers a different approach to the problem of quantum theory of gravity. In this framework gravity, Dark Energy (DE) and Dark Matter (DM) are seen as different manifestations of the quantum gravity. Astrophysical observations offer a unique test bed for gravitational theories since at large scales gravity is the dominant interaction. The equations of galactic and cosmic evolution arising from the Nexus Paradigm are tested against astrophysical observations which include, galaxy rotation curves, black hole observations by the Event Horizon Telescope and Advanced Ligo gravitational wave observations.

Acknowledgements

I would like to gratefully acknowledge the guidance and supervision from my supervisor and the support for my work I received from the department of Physics and Astronomy. I also acknowledge the support rendered by my family in realising this work.

Chapter 1

Introduction

This work deals with finding a plausible solution to three fundamental problems in physics namely Dark Energy (DE), Dark Matter (DM) and Quantum Gravity (QM) by testing the equations of the Nexus Paradigm of quantum gravity. This theoretical framework can be described as a quantized version of General Relativity GR in which DE and DM appear as low energy quantum corrections to the quantized version of GR.

A new fundamental particle of gravity – the Nexus graviton takes the centre stage in this paradigm. The Nexus graviton is a composite spin two particle of space-time with a Compton four wavelength that ranges from the Planck scale to the Hubble scale in integral increments of the Planck four-wavelength. This graviton is a spherically symmetric wave packet of four-space that does not execute translational motion but can only expand or contract via the emission or absorption of the ground state graviton. A test particle within the confines of the Nexus graviton experiences a Hubble flow with a flow velocity that obeys the Hubble law. The flow follows a curved path within the graviton and increases with increase in the graviton 4- radius as stipulated by Hubble's Law. The effects of the graviton become apparent at galactic and cosmic scales and therefore manifest as phenomena attributed to DM and DE. These properties of the Nexus graviton complete our picture of gravity resulting in the following universal law of gravity that applies from solar system to galactic and cosmic scales.

$$\frac{d^2r}{dt^2} = \frac{GM(r)}{r^2} + H_0 v_n - H_0 c \tag{1.1}$$

Therefore this work seeks to answer the following problem: **Are the equations of galactic evolution from the Nexus Paradigm of quantum gravity compatible with astrophysical observations?**

To this end, the **main objective** of this work is to test the above law of gravity at galactic scales using astrophysical observations such as galaxy rotation curve data.

Apart from giving a picture of the kinematics of matter at galactic and cosmic scales the Nexus Paradigm can describe gravity in the extreme regime of a black hole and black hole mergers. Therefore the **second objective** is to test the predictions of the Nexus model of

quantum gravity in the extreme gravity environment of black holes. The aLIGO observations therefore provide a unique opportunity to observe the dynamics of merging black holes and compare the observations with the predictions of the Nexus Paradigm. The Nexus Paradigm predicts that all merging black hole will merge with a relative speed slightly above half-light speed. For stellar mass black holes, mergers will take place at speeds almost exactly half the speed of light while for intermediate mass and supermassive black holes at speed slightly above half the speed of light due to the prevalence of strong perturbations with increase in mass. Neutron star mergers are predicted to occur at speeds no less than a quarter of the speed of light.

The radius of a black hole event horizon in the Nexus model is half of the magnitude predicted by GR. The Event Horizon Telescope will test this prediction by observing the silhouette of Sagittarius A*, the super massive black hole at the centre of the Milky Way, which will be half the size predicted by GR if the Nexus Paradigm is correct. A preliminary observation was published in May 2018 which shall be used to compare theory and observation. A final image will only be available by the second or third quarter of 2020.

Chapter 2

2. The Dark Sector

There are several known, unknowns in our understanding of the physical world as suggested by current astrophysical observations provided by a wide gamut of observational instruments at astronomy's disposal. These observations inescapably point out to the reality that vast amounts of Dark Matter (DM) and Dark Energy (DE) are necessary to account for the cosmic scale structures and cosmic acceleration. In this context, the adjective 'Dark' is synonymous to unknown. Strong evidence of these unknowns comes from the Planck 2013 (Ade *et al*. 2013*a*, 2013*b*) data and other sources (Baker *et al.*, 1999, Tegmark *et al* 2004, Komatsu *et al.* 2009) such as the Cosmic Microwave Background (CMB) radiation anisotropies, optical observations on supernovae Type Ia (Riess *et al.*, 1998, Permutter *et al*, 1999), galaxy rotational curves (Faber *et al.*,1976,) and galactic cluster dynamics (Vikhlinin *et al.*, Minchin *et al.*, 2005). Understanding the nature of DM and DE is a key challenge in modern astrophysics. This challenge is further compounded by the lack of direct detection of any material constituents of these phenomena by both space-based and ground-based experiments. Direct detection would undoubtedly reveal additional information on the nature and properties of DE and DM. This leaves astrophysical observations as the only available means of gathering information from which theoretical models are both built and tested.

In this work, I will discuss the limitations of current paradigms on DE and DM before introducing the Nexus Paradigm of quantum gravity as an alternative explanation of DE and DM.

2.1 Dark Energy and Limitations of current Dark Energy models

The total energy budget for the universe according to observations by the Planck 2013 mission, reveal that it consists of 4.9% ordinary matter, 26.8% DM and 68.3% DE. DE dominates the mass-energy of the universe and is widely accepted as the energy responsible for the observed accelerated cosmic expansion. The two most salient features of DE are homogeneous spatial distribution and a large negative pressure. These allow DE to be parametrized by its bulk equation of state

$$w = \frac{-P}{\rho} \tag{2.1}$$

here P is the pressure exerted by DE and ρ is the density of DE. Models that assume DE is some form of exotic energy are centred on the evolution of w. The equations of GR in their original form cannot lead to the observed acceleration and therefore need modification. This modification is done by either supplementing the energy momentum tensor with a DE component or modifying the geometrical description offered by these equations. This gives rise to a second set of models based on the modification of the geometry of space-time for large scale descriptions of the universe. Capozziello *et al.* (Capozziello *et al.* 2013) through the use of cosmographic techniques, have selected a number of leading models on the observed acceleration with the intention of finding the best-fit model. Their findings reveal that the leading DE models are as follows:

(1) The ΛCDM (Λ Cold Dark Matter) model;
(2) DE models with a constant equation of state (ωCDM or quintessence) , derived from a scalar field coupling with curvature;
(3) DE models in which the equation of state is parametrized in terms of the power of $a(t)$ as in for example the CPL parametrization;
(4) DE models that in which DE interacts with CDM as in the Chaplygin gas model;
(5) DE arising from quantum effects as in the Dvali–Gabadadze–Porrati (DGP) model and its phenomenological extension;
(6) $f(R)$-gravity theories;
(7) $f(T)$-gravity theories.

There are some models that interpret DE in terms of a barotropic fluid and this allows them to address the aspect that DE behaves anti-gravitationally but fail to explain the nature of a fluid that can give rise to such a negative pressure. The barotropic fluid is usually interpreted in terms of quantum vacuum energy which assumes the form of the cosmological constant Λ in Einstein's equation:

$$R_{\mu\upsilon} - \frac{1}{2}R g_{\mu\upsilon} + \Lambda g_{\mu\upsilon} = \frac{8\pi G}{c^4} T_{\mu\nu} \qquad (2.2)$$

The leading model in this genre of DE paradigms is the ΛCDM and fits the cosmological data well. However, the ΛCDM model in spite of its success is plagued with the serious problem of the orders of magnitude of the cosmological constant. Naive calculations for the vacuum energy contributions give a value 10^{120} orders of magnitude greater than the observed value of Λ. This is the so-called fine-tuning problem. Furthermore, the failure to

explain coincidence problem between the matter density and the cosmological constant is one other major theoretical shortcoming of the ΛCDM model. At galactic scales, the ΛCDM paradigm faces difficulties in providing a cogent description of galactic rotational curves, (Bullock & Boylan-Kolchin 2017, McGaugh 2014, Ferrero *et al* 2012, Van den Bosch & Swaters 2001) the core cusp problem (De Blok 2009, Navarro , Carlos & Eke 1996, Se-Heon O *et al* 2015) and the empirically observed baryonic Tully-Fisher relation (McGaugh 2011, 2005, Federico, McGaugh & Schombert 2015,). At cluster scales ΛCDM is confronted with challenges in describing the dynamics of the Bullet Cluster (Thompson, Dave & Nagamine 2014, Lee & Komatsu 2010) as well as the Abell 520 (Train Wreck) Cluster (Jee *et al* 2012,2014). These challenges, as well as the null detection of DM (Tan *et al* 2016 ,Akerib *et al* 2017, Cushman *et al* 2013, Sangalard *et al.* 2005) by both direct and indirect means have motivated other researchers to seek alternatives to the ΛCDM paradigm. The alternatives should not only address these challenges but explain the success of GR at solar system scales as well.
In a bid to remedy these shortcomings, several models such as models (2)–(5) have been proposed. However, none of them is fully satisfactory, from both theoretical and observational points of view.

$f(R)$ theories (Capozziello S *et al* 2002, Chiba T *et al* 2007,Olmo G. J. 2005) are models attempting to explain the DE phenomenon via the modification of the geometric description of General Relativity (GR). The simplest is the Starobinsky model for inflation (Starobinsky 1979) for which the Ricci scalar becomes $f(R) = R + \alpha R^2$. These models have been successful in describing the temperature anisotropies in the CMB. Furthermore an application of these models at both solar system and galactic system scales offer viable alternatives to DM. There are other extensions to GR that exist in the form of $f(T)$ theories in which gravity is interpreted as a torsion and the dynamic equations give descriptions of particle trajectories which are governed by a gauge gravitational field. The applications of $f(T)$ theories in relation to cosmic expansion have been studied in length by (Dent J B 2011 ,Setare M R 2013, Bamba K *et al* 2012, Wu P *et al* 2010, Li B *et al* 2011) The main disadvantage of both $f(R)$ and $f(T)$ theories is that the correct modifications of GR are unknown *a priori*.

2.2 Dark Matter and limitations of current Dark Matter models

The "missing mass" problem in galactic and galactic cluster dynamics was first postulated by Jans Oort in 1932 and by Fritz Zwicky in 1933. In 1937, Zwicky (Zwicky 1937) provided the first reproducible evidence of the presence of unseen matter in the Coma Cluster group of galaxies by applying the classic virial theorem. This 'missing mass' is today known as DM and its nature is one of the greatest puzzles in astrophysics. The advent of precision cosmology has permitted increasingly detailed studies of CMB anisotropies which has provided further convincing evidence for the abundance of DM . The latest precision measurements of the CMB are from the Planck satellite mission. These new measurements are in good agreement with predictions from the ΛCDM model, in which the cosmos is dominated by DE(Λ) and CDM.

CDM is hypothesized as particulate non-baryonic matter that interacts with ordinary matter mostly gravitationally. There are several suggested candidates for the CDM. The leading candidates are the so called Weakly Interactive Massive Particles (WIMPs) . These are Supersymmetric particles that are hypothesized to interact with baryonic matter via the weak nuclear force (Goodman M and Witten E 1985) and also via the gravitational interaction. WIMPs are hypothetical neutral particles and moving at non-relativistic velocities and are predicted to interact weakly mainly with an atomic nucleus, whose nuclear recoil energy can be measured by a DM detector. There are several direct detection experiments (Sangalard V *et al. 2005*, Archambault S *et al* 2009, Aalseth C 2011, LUX Collaboration 2013,) that have been set up based on this theoretical assumption. To date no WIMP has been detected as shown by the null result from several direct detection experiments (Cui X 2017). The Panda X experiment is the most sensitive so far and has put stringent limits on the energies of these hypothetical particles and hence narrowed the search.

There are other possible DM candidates apart from WIMPs. The most favoured after WIMPs are the so-called axions and arise from theoretical predictions of the Peccei–Quinn symmetry which is an attempt to explain why the strong nuclear interaction obeys CP symmetry. The axion is predicted to be a stable subatomic particle having a mass less than 1 eV making it lighter than a WIMP particle and therefore much harder to detect. Several other exotic candidates have been proposed such as gravitinos, WIMPzillas etc. all which require direct detection to be confirmed. Furthermore, it is not sufficient to detect

these particles in particle colliders but more importantly, that these particles must be detected behaving as DM to be considered as the source of DM.

There are models that suggest that the DM phenomenon may arise from a modification of the law of gravity. In this framework galactic and galactic cluster dynamics could be explained by assuming that GR is incomplete and requires modifications for large scale descriptions. This is where $f(R)$ theories come in. The simplest modified theory of gravity is MoND (Modified Newtonian Dynamics) (Milgrom M 1983) and its relativistic version TeVeS (Berkenstein J D 2011). MoND has excelled in explaining galactic rotational curves and the dynamics of dwarf galaxies better than the ΛCDM model [Sanders R H et al 2002, Famaey B and McGaugh S S 2012, Milgrom M and McGaugh S S 2013). MoNDian theories have shortcomings when it comes to describing large scale galactic cluster dynamics wherein the ΛCDM model reigns supreme.

In light of these shortcomings there is a plethora of $f(R)$ theories designed to remedy the issues but as noted above, $f(R)$ theories have the disadvantage that the desired correct modifications to GR are unknown *a priori*.

2.3 Toward a quantum cosmological solution

In synthesis, the ΛCDM model satisfactorily describes DE to a degree which is in close agreement with observation and finding a solution to the fine-tuning and the coincidence problems would bring our understanding of DE closer to completion. On the other hand, Extended Theories of Gravity and in particular MoND model DM with greater accuracy than the ΛCDM model especially at galactic scales. These observations lead one to intuitively imagine a comprehensive model in which GR is modified while at the same time the cosmological constant is retained. Currently DM is known to interact gravitationally. This known fact alone could suggest that a DM particle is a particle of gravity— the hypothetical graviton. Kiefer (Kiefer C 2013, Kiefer C and Kramer M 2012) suggests that a quantum approach to cosmology is relevant to an understanding of the real universe. This approach demands quantum gravity since gravity is the dominant interaction at such large scales. A number of quantum gravity theories are being extended to cover the cosmological scales since these scales might serve as testing ground for quantum gravity theories using simple mathematical terms.

Chapter 3

3. The Problem of Quantum Gravity

At present, physical phenomena are explained through either summoning the explanatory power of QM or GR. Elementary particles and molecules as well as the weak nuclear force, the strong nuclear force and the electromagnetic interaction are elegantly described by the QM. The fundamental concept at the core of QM is the wave function, which through the Born rule affords an explanation of microcosmic phenomena. GR is a classical theory which explains gravity, the dominant interaction at macrocosmic scales, in terms of the geometry of space-time itself. Since the fundamental concept in GR is the description of gravity using the language of geometry of spacetime and that of QM is the esoteric wave function then the problem of QG is therefore to seek a description of gravity in terms of the principles of QM. To seek a geometric description of the microworld using GR is impossible since at this level GR yields infinities, which are a sure signal that the theory has reached its limits. On the other hand QM can provide insights on the properties of space-time at infinitesimal spacetime intervals. A direct attempt to apply the rules of QM to the problem of gravity at small scales yields infinities upon infinities, a situation which is much absurd than applying GR. Gravity therefore seems non quantizable and only accepting a classical geometric description.

The path to reconciling GR with QM as suggested by the author, require considering the following aspects:

1. GR is preferably interpreted as a theory of straight lines in curved spacetime and yet Einstein's equations can also be interpreted as curved lines in flat spacetime. By adopting the latter interpretation, one can start embarking on an alternative path to quantum gravity since QM is a theory built on flat spacetime and has curved lines that appear as sum over histories in the Feynman interpretation of QM. Moreover the Ricci tensor in GR is the average of the possible paths a test particle can take in a gravitational field.
2. Secondly the non-localizability of gravitational energy hints at the Uncertainity Principle providing an important role in formulating a self-consistent quantum theory of gravity.

Before one can start developing a self-consistent QG theory, it is important to consider the current approaches to this problem and their limitations

3.1 Limitations of current approaches to Quantum Gravity

There is a plethora of proposals for quantum gravity theories and yet none are close to resolving completely the problem of quantum gravity. This is because candidate theories need to resolve major conceptual and formal problems. Moreover, these models make predictions that are beyond the reach of experimental tests.

3.2 Other approaches to Quantum Gravity

There exist various approaches to quantum gravity which differ depending on which aspects of GR and QM they assimilate without changes and other features which they assimilate with modifications. Below is a list of some popular approaches to the problem of quantum gravity.

3.2.1 Asymptotically safe Quantum Gravity

Asymptotic safety (Percacci R 2007, Eichhorn A 2017) starts from using nontrivial renormalization group fixed points to simplify the procedure of perturbative renormalization. In this approach, the couplings tend to approach finite values at high energies and the running coupling constants remain finite. This condition is sufficient to avoid unphysical divergences in scattering amplitudes.

3.2.2 Euclidean Quantum Gravity

The Euclidean approach to quantum gravity (Gibbons GW and Hawking SW 1993) is a version of quantum gravity which is Wick rotated and formulated as a quantized field theory. In this formulation, compact Riemannian manifolds in four dimensions are used instead of pseudo Riemannian manifolds. These manifolds are connected and boundaryless.

3.2.3 Causal dynamical triangulation

Causal dynamic triangulation (Ambjorn J 2013) is a modified version of Regge calculus in which space-time is quantized by a triangulation process. This formulation considers a

space-time of n-dimensions as constituted from slices of space that are labelled by a quantized time variable *t*.

3.2.4 Causal fermion systems

This formulation is premised on that the negative energy solutions of the Dirac equation in Minkowski space are part of to the Dirac sea (Finister F 2016). This approach to quantum gravity considers that the wave functions of all occupied states as the basic physical objects. Structures in 4-space arise as a consequence of the interaction of sea states with each other and as well as interactions with the extra particles and "holes" in the sea.

3.2.5 Causal sets

The founding principles of the Causal sets (Reid DD 1999) program are that space-time is a collection of discrete space-time points and that these points are causally connected by a partial order. The partial order provides causality relations between space-time events and is based upon a theorem by David Malament (Malament DB 2000) which states that a conformal isomorphism map can be defined as a bijective map between a pair of past and future distinguishing space-times that preserves their causal structure.

3.2.6 Group field theory

Group field theory (Friedel L 2005) is closely related to LQG and causal dynamic triangulation . In this model the basic manifold is a Lie group. Spin foams and simplicial pseudo-manifolds form its perturbative expansion and its partition function defines a non-perturbative sum over all geometries and topologies. This yields a path integral formulation of quantized space-time.

3.2.7 Wheeler–DeWitt equation

This field equation was first proposed by Bryce DeWitt (DeWitt 1967) and is an approach in which the Hamilitonian does not evolve in time, leading to the so-called 'problem of time' (Anderson E 2010). The formulation is also plagued with conceptual issues such as the precise definition and meaning of the wave function of the universe.

3.2.8 Geometrodynamics

Geometrodynamics (Anderson E 2004) describes space-time and associated phenomena completely in terms of geometry. Its aims to reformulate GR in a framework consisting of three-metrics and modulo three-dimensional diffeomorphisms.

3.2.9 Hořava–Lifshitz gravity

This approach to the problem of quantum gravity was first proposed by Petr Hořava in 2009 (Wang A 2017).

attempts to give a deeper conceptual understanding of time in QM and GR by assuming that space and time are not equivalent at high energiesor short distances and that the relativistic concept of time emerges at large scales. The drawback is that the speed of light becomes infinite at high energies. Concepts such as critical phenomena in condensed matter physics are employed in this model which relies on the theory of foliations to produce its causal structure.

3.2.10 Regge calculus

Regge calculus formalism in GR is used for simplifying solutions to GR. This calculus method was first introduced in 1961(Immirzi G 1997) by the Italian theoretician Tullio Regge and has been successfully applied to simulate colliding black hole binaries.The axiomatic principle in Regge's work is arises from the fact that every Lorentzian manifold admits a triangulation into simplices and that the space-time curvature can be expressed in terms of deficit angles associated with 2-faces where arrangements of 4-simplices meet. Regge showed that Einstein’s vacuum field equations can be reformulated as a restriction on these deficit angles. Regge calculus is equivalent to saying that the Riemann curvature tensor can be computed from the metric tensor of a Lorentzian manifold.

.

3.2.11 Scale relativity

This approach is based on fractal space-time theory (Nottale L 2008). Scale relativity theory attempts to extend GR to physical scales using fractal geometries and introducing the concept of "state of scale".The model is still yet to be developed to a full general scale relativity.

3.2.12 Shape Dynamics

This approach is founded on Machian principle. It is equivalent to the ADM formalism (Herczeg G 2017) . It salient feature of the approach is the resolution of the problem of time by replacing space-time with an evolving spatial conformal geometry.

3.2.13 Superfluid vacuum theory

Superfluid vacuum theory (Volovik GE 2000), is an approach which considers space-time as a Bose–Einstein condensate. Though, the microscopic structure of this physical vacuum is currently unknown SVT aims to ultimately to explain all fundamental forces of nature through this approach.

3.2.14 Supergravity

Supergravity theory (Deser S 2017) is a field theory that combines the axioms of supersymmetry and GR. Here, supersymmetry is considered as a local symmetry. The generators of supersymmetry (SUSY) are convoluted with the Poincaré group to form a super-Poincaré algebra which implies that supergravity follows naturally from local supersymmetry.

3.2.15 Twistor theory

This approach wasfirst proposed by Sir Roger Penrose in 1967,(Atiyah M 2017). In this model, Minkowski space is transformed into twistor space by means of the Penrose transfom. Twistors are specified complex coordinates. The Penrose transform transforms geometric objects from a four space of Hermitian signature (2,2) into geometric objects in twistor space.

3.2.16 Canonical quantum gravity

This is an attempt to quantize the canonical formulation of GR. It is a Hamiltonian formulation of GR first outlined by Bryce DeWitt (DeWitt 1967) in 1967, using canonical quantization techniques for constrained Hamiltonian systems invented by P.A.M. Dirac.

3.2.17 E8 Theory

Garrett Lisi developed this theory with the goal to describe all particle fields as part of the E8 Lie algebra.(Lisi AG 2007)

This theory is part of theories of the grand unified theory program. The theory has a geometric approach to the unification of fundamental forces of nature and is still a work in progress.

3.2.18 A synopsis of approaches to Quantum Gravity

In synthesis, as already noted above, there is no currently accepted self- consistent quantum theory of gravity. Most approaches, if not all, are confronted with both conceptual and mathematical challenges which are difficult to resolve. The absence of experimental observation of quantum gravity phenomenology has left the field with no concrete direction to pursue.

Chapter 4

4 The fundamentals of the Nexus Paradigm of quantum gravity

4.1 The Nexus Graviton

The prime focus of this chapter is on the conceptual foundations of the Nexus Paradigm of quantum gravity which distinguishes it from the other approaches mentioned in the previous chapter.

This formulation starts from the premises that in physics the primary objective is to find functional relationships amongst measurable physical quantities. In particular, a unifying paradigm of physical phenomena should reveal the functional relationship between the fundamental physical quantities of 4-space and 4-momentum. At present, GR and QM offer the best predictions of the results of measurement of physical phenomena using different languages. GR describes nature in the language of geometry while QM employs the language of wave functions. The problem of quantum gravity is therefore to interpret GR in terms of the wavefunctions of QM. Translating the language of measurement of GR into that of QM becomes the primary objective of the Nexus formulation of quantum gravity.

For a free falling observer, measurements in GR take place in a local patch of spacetime which can be considered as a flat Minkowski space. The line element in Minkowski space which is the subject of measurement, can be computed through the inner product of the local coordinates as

$$\Delta x^{\mu}\Delta x_{\mu} = \Delta x^2 + \Delta y^2 + \Delta z^2 - c^2\Delta t^2$$
$$= (A\Delta x + B\Delta y + C\Delta z + iDc\Delta t)(A\Delta x + B\Delta y + C\Delta z + iDc\Delta t) \quad (4.1.1)$$

If one multiplies the right hand side one notes that to make all the cross terms such as $\Delta x\Delta y$ to cancel out one must make the following assumption:

$$AB + BA = 0 \; A^2 = B^2 = \cdots = 1 \quad (4.1.2)$$

The above conditions therefore imply that the coefficients (A, B, C, D) generate a Clifford algebra and therefore must be matrices. These coefficients can be re-written in the 4-tuple

form as $(\gamma^1, \gamma^2, \gamma^3, \gamma^0)$ which may be summarized using the Minkowski metric on spacetime as follows

$$\{\gamma^\mu, \gamma^\nu\} = 2\eta^{\mu\nu} \tag{4.1.3}$$

The gammas are of course the Dirac matrices. Thus one can express a displacement 4-vector as

$$\Delta x^\mu = r_{HS}\gamma^\mu \tag{4.1.4}$$

Where r_{HS} is the Hubble radius. Here the Hubble diameter is considered as the maximum dimension of the local patch of space since it is physically impossible to interact with objects beyond the Hubble 4- radius. It is important to note that the line element is the square of the amplitude of the displacement 4-vector. Thus in order to express GR in terms of the language of QM one must make the radical assumption that the displacement vectors in Minkowski space are pulses of 4-space which can be expressed in terms of Fourier functions as follows

$$\Delta x_n^\mu = \frac{2r_{HS}}{n\pi}\gamma^\mu \int_{-\infty}^{\infty} sinc(kx)e^{ikx}dk$$

$$= \gamma^\mu \int_{-\infty}^{\infty} a_{nk}\varphi_{(nk)}dk \tag{4.1.5}$$

Where $$\frac{2r_{HS}}{n\pi} = \sum_{k=-\infty}^{k=+\infty} a_{nk} \tag{4.1.6}$$

Here $\varphi_{(nk)} = sinc(kx)e^{ikx}$ are Bloch energy eigenstate functions.The Bloch functions can only allow the four wave vector to assume the following quantized values

$$k^\mu = \frac{n\pi}{r_{HS}^\mu} \quad n = \pm 1, \pm 2 \ldots 10^{60} \tag{4.1.7}$$

The minimum 4-radius in Minkowski space is the Planck 4- length since it is impossible to measure this length without forming a black hole. The 10^{60} states arise from the ratio of Hubble 4-radius to the Planck 4-length.The displacement 4-vectors in each eigenstate of space-time generate an infinite Bravias 4-lattice. Also, condition (4.1.7) transforms Eqn.(4.1.5) to

$$\Delta x_n^\mu = \gamma^\mu \int_{-nk_1}^{nk_1} a_{nk}\varphi_{(nk)}dk \tag{4.1.8}$$

The second assumption of the Nexus formulation of quantum gravity is that each displacement 4- vector is associated with a conjugate pulse of four momentum which can also be expressed as a Fourier integral

$$\Delta p_n = \frac{2np_1}{\pi}\gamma_\mu \int_{-nk_1}^{nk_1} \varphi_{(nk)} dk$$

$$= \gamma_\mu \int_{-nk_1}^{nk_1} c_{nk}\varphi_{(nk)} dk \qquad (4.1.9)$$

Where $p_1$is the four momentum of the ground state.

A displacement 4-vector and its conjugate 4-momentum satisfy the Heisenberg uncertainty relation

$$\Delta x_n \Delta p_n \geq \frac{\hbar}{2} \qquad (4.1.10)$$

The Uncertainty Principle plays the important role of generating a vector bundle, out of the total uncertainty space *E* of trivial displacement 4-vectors from which a closed compact manifold *X* is formed i.e($\pi: E \rightarrow X$). Each point on the manifold is associated with a vector which is along a normal to the manifold. In other words the Uncertainty Principle causes variations in the geodesic path which generates a set of curve linear trajectories within the local flat patch of spacetime. These trajectories are best described by a curved coordinates system within the local flat patch. This curved coordinate system explains why a ray of light traces a curved trajectory as seen by a free falling observer in his local frame of reference.

The wave packet described by Eqn.(4.1.8) is essentially a particle of four-space. The spin of this particle can be determined from the fact that a component the four displacement vector will transform according to the law

$$\Delta x'^{\mu}_n = \exp(\frac{1}{8}\omega_{\mu\upsilon}[\gamma_\mu, \gamma_\upsilon])\Delta x^{\mu}_n \qquad (4.1.11)$$

Where $\omega_{\mu\upsilon}$ is an antisymmetric 4x4 matrix providing the parameterization of the transformation.

Thus, a component of the four vector has a spin half. A summation of all the four half spins yields a total spin of *2.* The name ‘ Nexus graviton’ is given to this particle of 4-space since the primary objective of quantum gravity is to find the nexus between the concepts of GR and QM.

From Eqn.(4.1.7) the norm squared of the 4- momentum of the *n*-th state graviton is

$$(\hbar)^2 k^{\mu} k_{\mu} = \frac{E_n^2}{c^2} - \frac{3(nhH_0)^2}{c^2} = 0 \tag{4.1.12}$$

where H_0 is the Hubble constant ($2.2 \times 10^{-18}\ s^{-1}$) and can be expressed in terms of the cosmological constant, Λ as

$$\Lambda_n = \frac{E_n^2}{(hc)^2} = \frac{3k_n^2}{(2\pi)^2} = n^2\Lambda \tag{4.1.13}$$

One can infer from Eqn.(4.1.13), that the Nexus graviton (or displacement 4-vector) in the *n*-th quantum state forms a trivial vector bundle via the Uncertainty Principle which generates a compact flat manifold which consists of curve linear coordinates of positive Ricci curvature that can be expressed in the form

$$G_{(nk)\mu\upsilon} = n^2\Lambda g_{(n,k)\mu\upsilon} \tag{4.1.14}$$

where $G_{(nk)\mu\nu}$ is the Einstein tensor of space-time in the *n*-th state. Eqn.(4.1.14) depicts a contracting geodesic ball and as explained in (Marongwe 2015) this is DM which is an intrinsic compactification of the elements space-time in the *n*-th quantum state. This compactification is a result of the superposition of several plane waves as described by Eqn.(4.1.8) to form an increasingly localized wave packet as more waves are added. Similary the converse is also true. The loss of harmonic waves expands the elements of spacetime which gives rise to DE. Thus the DE arises from the emission of a ground state graviton such that Eqn.(4.1.14) becomes

$$G_{(nk)\mu\upsilon} = (n^2 - 1)\Lambda g_{(n,k)\mu\upsilon} \tag{4.1.15}$$

These are Einstein's vacuum field equations in the quantized spacetime.If the graviton field is perturbed by the presence of baryonic matter then Eqn.(15) becomes

$$\begin{aligned} G_{(nk)\mu\upsilon} &= kT_{\mu\nu} + (n^2 - 1)\Lambda g_{(n,k)\mu\upsilon} \\ &= kT_{\mu\nu} + (n^2 - 1)k\rho_{DE} g_{(n,k)\mu\upsilon} \end{aligned} \tag{4.1.16}$$

Where ρ_{DE} is the density of DE.

It is important to keep in mind that in the Nexus Paradigm, unlike in GR, Eqn(4.1.16) is interpreted as describing curved world lines in a flat spacetime.

4.2 The Schwarzschild Solution

In this section the field equations describing a Nexus graviton are solved following Karl Schwarzschild as described in (Marongwe 2015) to find the space-time geometry associated stationary, spherical distribution ($r_n = r_{HS}/n$) of vacuum matter of mass:

$$M_{vac} = \frac{n^2c^4}{8\pi G}\Lambda \int_0^{V_n} dV_n \tag{4.2.1}$$

Since the space outside the Nexus graviton event is empty, the energy-momentum tensor $T_{\mu\nu}$ vanishes, so the field equation becomes:

$$G_{\mu\nu} = 0 \tag{4.2.2}$$

The appropriate boundary conditions are:

• metric must match interior metric at the body's surface;

• metric must assume the form of a flat (Minkowski) metric far away from the body.

This is the Schwarzschild problem which is solved by solving for the Schwarzschild metric $g_{\mu\nu}$ starting from a consideration of a general static and isotropic metric:

• *static*: both time-independent and symmetric under time reversal;

• *isotropic*: invariant under spatial rotations.

The interval satisfying these criteria may be written as:

$$ds^2 = A(r)dt^2 + B(r)dr^2 + r^2d\theta^2 + \sin^2\theta d\varphi \tag{4.2.3}$$

where the first two terms on the right-hand side describe radial behaviour (isotropy), and the last two the surface of the sphere (spherical symmetry). It can be expressed in many equivalent forms. One convenient form is:

$$ds^2 = e^{N(r)}dt^2 + e^{P(r)}dr^2 + r^2(d\theta^2 + \sin^2\theta d\varphi^2). \tag{4.2.4}$$

The Schwarzschild problem is now reduced to solving for $N(r)$ and $P(r)$ from the field equations and the appropriate boundary conditions. Following Schwarzschild, the solution to the Schwarzschild problem is

$$ds^2 = -\left(1 - \left(\frac{2GM_{vac}}{c^2r}\right)\right)c^2dt^2 + \left(1 - \left(\frac{2GM_{vac}}{c^2r}\right)\right)^{-1}dr^2 + r^2(d\theta^2 + sin^2\theta d\varphi^2) \tag{4.2.5}$$

Given that $v = H_0r$ and that

$$\frac{GM_{vac}}{r} = v^2 = (H_0r)^2 \tag{4.2.6}$$

then the Schwarzschild solution for the Nexus graviton reduces to

$$ds^2 = -\left(1 - \left(\frac{2(H_0r)^2}{c^2}\right)\right)c^2dt^2 + \left(1 - \left(\frac{2(H_0r)^2}{c^2}\right)\right)^{-1}dr^2 + r^2(d\theta^2 + sin^2\theta d\varphi^2) \tag{4.2.7}$$

Also given that $n^2 = \left(\frac{H_0}{cr}\right)^2 = \left(\frac{r_{HS}}{r}\right)^2$

then Eq. (4.6.7) can be written as

$$ds^2 = -\left(1 - \left(\frac{2}{n^2}\right)\right)c^2dt^2 + \left(1 - \left(\frac{2}{n^2}\right)\right)^{-1} dr^2 + r^2(d\theta^2 + sin^2\theta d\varphi^2) \quad (4.2.8)$$

The above metric describes a curved worldline on a flat spacetime.

4.3 Interpretation of the Solutions

One prominent feature of Eq. (4.2.8) is asymptotic straightness of worldliness such that at the Planck state ($n = 10^{60}$) the metric reduces to a straight line in flat Minkowski space

$$ds^2 = -c^2dt^2 + dr^2 + r^2(d\theta^2 + \sin^2\theta d\varphi^2) \quad (4.3.1)$$

This implies that at high energies the world line does not deviate from a linear trajectory because the uncertainities in its 4-position are negligible. The metric begins to deviate substantially at low energies wherein the uncertainities in its 4-position are large. Thus gravity is a low energy phenomenon wherein the world line becomes degenerate.

A more remarkable feature of the same equation is the lack of a singularity which is present in classical GR at the quantum state (n =1) i.e. at the Hubble radius. In this quantum state the metric undergoes a signature change and the line element becomes also flat:

$$ds^2 = c^2dt^2 - dr^2 + r^2(d\theta^2 + \sin^2\theta d\varphi^2) \quad (4.3.2)$$

4.4 Dependence of frequency redshifts and time dilation with radial distances

Gravitons of large four-wave vector have infinitesimal line elements in line with the Uncertainty Principle. This results in an equally infinitesimal proper motion $v = \pi H_0/kn$ of a test particle placed at a radial distance $r = \pi/kn$ within the graviton, compared to a test particle placed in gravitons of small four-wave vector. Thus at radii approaching the Planck length, motion in the classical sense is imperceptible. A comparison of relative motion at different radii can be made by comparing the redshift of light emitted by an atom within a graviton of radius $r + D$ to that emitted by an atom within a graviton of radius r. Applying the Schwarzschild solution for gravitational redshift and time dilation to the Nexus paradigm, the wavelength of light at r, λ_r compared to the wavelength at $r + D$,

$$\lambda_{r+D} = \lambda_r \sqrt{\frac{1-\frac{2r^2}{r_{HS}^2}}{1-\frac{2(r+D)^2}{r_{HS}^2}}} \qquad (4.4.1)$$

Time dilation occurs at large radii of the graviton compared to small radii and is the cause of the redshift. The time transitions at (r +D) compared to those at r is therefore:

$$\tau_{r+D} = \tau_r \sqrt{\frac{1-\frac{2r^2}{r_{HS}^2}}{1-\frac{2(r+D)^2}{r_{HS}^2}}} \qquad (4.4.2)$$

We infer from the above expression that when the universe was younger, it aged faster. The existence of stellar objects, lenticular galaxies and large-scale structures that seem older than the universe has been the subject of much debate threatening the validity of the Big Bang model. We cite these cosmic misfits as evidence of a fast-aging cosmic epoch in the early universe as inferred from Eqn.(4.4.2).

4.5 The Extended Solution

A the solution which includes baryonic matter of mass M_{bar} as described by Eqn.(4.1.16)

$$G_{(n)\mu\upsilon} = kT_{\mu\nu} + (n^2-1)\Lambda g_{\mu\upsilon}$$

is as follows:

$$s^2 = -\left(1-\left(\frac{2G(M_{bar}+M_{vac})}{c^2 r}-\left(\frac{2GM_\Lambda r}{c^2 r_{HS}^2}\right)\right)\right)c^2dt^2+\left(1-\frac{2G(M_{bar}+M_{vac})}{c^2 r}-\left(\frac{2GM_\Lambda r}{c^2 r_{HS}^2}\right)\right)^{-1}dr^2+$$
$$r^2(d\theta^2+sin^2\theta d\varphi^2) \qquad (4.5.1)$$

The term $\frac{GM_\Lambda r}{r_{HS}^2}$ is the work done per unit mass in moving a test particle a distance r by a constant force field $\frac{GM_\Lambda}{r_{HS}^2}$. This constant force field is generated by the emission of a ground state graviton each time a Nexus graviton expands. In the weak field limit Eqn. (4.5.1) becomes:

$$ds^2 = -\left(1-\left(\frac{2G(M_{bar}+M_{vac})}{c^2 r}-\left(\frac{2GM_\Lambda r}{c^2 r_{HS}^2}\right)\right)\right)c^2dt^2+\left(1-\frac{2G(M_{bar}+M_{vac})}{c^2 r}+\right.$$
$$\left.\left(\frac{2GM_\Lambda r}{c^2 r_{HS}^2}\right)\right)dr^2+r^2(d\theta^2+sin^2\theta d\varphi^2) \qquad (4.5.2)$$

Implementing the non-relativistic velocity requirement by taking the limit $v/c \rightarrow 0$. reduces Eqn. (4.9.11) to

$$ds^2 = -\left(1 - \left(\frac{2G(M_{bar} + M_{vac})}{c^2 r} - \left(\frac{2GM_\Lambda r}{c^2 r_{HS}^2}\right)\right)\right)c^2dt^2 + dr^2 + r^2(d\theta^2 + sin^2\theta d\varphi^2) \quad (4.5.3)$$

. The resulting geodesic line for a test particle in this field is determined by the

following differential equations:

$$\frac{d^2x^\lambda}{d\tau^2} + \Gamma^\lambda_{\mu\nu}\frac{dx^\mu}{d\tau}\frac{dx^\nu}{d\tau} = 0 \quad (4.5.4)$$

By converting Eqn. (4.5.4) to the Cartesian form:

$$ds^2 = -\left(1 - \left(\frac{2G(M_{bar} + M_{vac})}{c^2 r} - \left(\frac{2GM_\Lambda r}{c^2 r_{HS}^2}\right)\right)\right)c^2dt^2 + dx^2 + dy^2 + dz^2, \quad (4.5.5)$$

we are able to conveniently calculate the Christoffel symbols $\Gamma^\lambda_{\mu\nu}$ from which we obtain the final expression as

$$\frac{d^2r}{dt^2} - \frac{G(M_{bar} + M_{vac})}{r^2} + \frac{GM_\Lambda}{r_{HS}^2} = 0 \quad (4.5.6)$$

Given that

$$\frac{GM_{vac}}{r^2} = \frac{v^2}{r} = \frac{(H_0 r)^2}{r} = H_0 v \quad (4.5.7)$$

and that

$$\frac{GM_{vac}}{r_{HS}^2} = \frac{c^2}{r_{HS}^2} = \frac{(H_0 r_{HS})^2}{r_{HS}^2} = H_0 c \quad (4.5.8)$$

Therefore in the weak field, the gravitational acceleration is

$$\frac{d^2r}{dt^2} = \frac{GM(r)}{r^2} + H_0 v_n - H_0 c \quad (4.5.9)$$

Here the last two terms refer to the acceleration contributions due to DM and DE respectively.

4.6 The new Schwarzschild radius

A further interpretation of Eqn. (4.2.8) reveals that the state of maximum space-time curvature occurs when n=1 such that

$$r_{NS} = \frac{GM(r)}{c^2} \quad (4.6.1)$$

is the minimum radius of curvature or the new Schwarzschild radius (r_{NS}) which is half the classical Schwarzschild radius in GR. No test particle will fall below this radius suggesting that nothing falls into a black hole and hence no information is lost.

4.7 Canonical transformations in the Nexus Paradigm.

In classical mechanics, a system is described by n independent coordinates (q_1, q_2,...q_n) together with their conjugate momenta (p_1,p_2,...p_n). In the Nexus Paradigm, the labeling q_n refers to a creation of a Nexus graviton in the n-th quantum state associated with a conjugate momentum p_n . The Hamiltonian equation

$$\dot{q}_n = \frac{\partial H}{\partial p_n} \tag{4.7.1}$$

refers to the rate of expansion or contraction of space-time generated by the graviton creation or annihilation operations and

$$\dot{p}_n = -\frac{\partial H}{\partial q_n} \tag{4.7.2}$$

refers to the force field associated with the graviton creation or annihilation. It is important to note that this force field generates an isotropic expansion or contraction of space-time within the spatio-temporal dimensions of the graviton.

We can also rewrite the Hamiltonian equations in terms of Poisson brackets which are invariant under canonical transformations as

$$\dot{q}_n = \{q_n, H\} \quad , \quad \dot{p}_n = \{p_n, H\} \tag{4.7.3}$$

The Poisson brackets provide the bridge between classical and quantum mechanics (QM) and in QM, these brackets are written as

$$\dot{\hat{q}}_n = \left[\hat{q}_n, \hat{H}\right] \quad , \quad \dot{\hat{p}}_n = [\hat{p}_n, \hat{H}] \tag{4.7.4}$$

and obey the following commutation rules

$$[\hat{q}_n, \hat{q}_s] = 0 \ , \ [\hat{p}_n, \hat{p}_s] = 0 \ , \ [\hat{q}_n, \hat{p}_s] = \delta_{ns} \tag{4.7.5}$$

4.8 The Hamiltonian formulation for the quantum vacuum

The Nexus graviton is a pulse of space-time which can only expand or contract and does not execute translational motion implying that the Hamiltonian density of the system is equal to the Lagrangian density.

$$H = L \tag{4.8.1}$$

GR is a metric field in which the energy density in four space determines its value. Since the Bloch energy eigenstate functions determine the energy of space-time, it is therefore imperstive to express the metric in terms of the Bloch wave functions. Since the eigenstate four space components of the Nexus graviton in the *k*-th band are

$$\Delta x_{nk}^{\mu} = z_{nk}^{\mu} = a_{nk}\gamma^{\mu} sinc(kx)e^{ikx} \tag{4.8.2}$$

then an infintesimal four radius within the *k*-th band is computed as

$$dr_{nk}^{\mu} = \frac{\partial z_{n,k}^{\mu}}{\partial k^{\mu}} dk^{\mu} = ix_{\mu}a_{nk}\gamma^{\mu} sinc(kx)e^{ikx}dk^{\mu} \tag{4.8.3}$$

In Eqn.(4.8.3) the first order derivative of the periodic sinc function is equal to zero for all integral values of *n*.

The interval within the band is then computed as

$$\begin{aligned} ds^2 = dr_{nk}^{\mu}dr_{nk}^{\mu} &= \frac{\partial z_{n,k}^{\mu}}{\partial k^{\mu}}\frac{\partial z_{n,k}^{\mu}}{\partial k^{\nu}} dk^{\mu}dk^{\nu} \\ &= b_{\mu}c_{\nu}\gamma^{\mu}\varphi_{(n,k)}\gamma^{\nu}\varphi_{(n,k)}dk^{\mu}dk^{\nu} \end{aligned} \tag{4.8.4}$$

Here the interval is described in terms of the reciprocal lattice and $b_{\mu} = ix_{\mu}a_{nk}$ and $c_{\mu} = ix_{\mu}a_{nk}$. The metric tensor of four space in the *k*-th band is therefore associated with the Bloch energy eigenstate functions of the quantum vacuum as follows

$$\begin{aligned} g_{(n,k)\mu\nu} &= \gamma_{\mu}\gamma_{\nu}\varphi_{(n,k)}\varphi_{(n,k)} \\ &= \eta_{\mu\nu}\varphi_{(n,k)}\varphi_{(n,k)} \end{aligned} \tag{4.8.5}$$

The Lagrange density for Eqn. (4.1.16) following Einstein and Hilbert is

$$L_{EH} = k(R - 2(n^2 - 1)\Lambda) \tag{4.8.6}$$

Given that the Einstein tensor in a compact manifold is equal to the Ricci flow

$$-\partial_t g_{\mu\nu} = \Delta g_{\mu\nu} = R_{\mu\nu} - \frac{1}{2} R g_{\mu\nu} = G_{\mu\nu} \tag{4.8.7}$$

The equations of motion of the quantum vacuum obtained from Eqn.(4.7.6) yield the following quantized field equations

$$-\partial_t(\gamma_\mu \varphi_{(n,k)} \gamma_\nu \varphi_{(n,k)}) = (n^2 - 1)\Lambda(\gamma_\mu \varphi_{(n,k)} \gamma_\nu \varphi_{(n,k)}) \tag{4.8.8}$$

which can be written as

$$\partial_t(\gamma_\mu \varphi_{(n-1,k)} \gamma_\nu \varphi_{(n+1,k)}) = \frac{-i^2}{(2\pi)^2} \gamma_\mu \nabla \varphi_{(n-1,k)} \gamma_\nu \nabla \varphi_{(n+1,k)}$$

$$= \frac{1}{4\pi^2} \gamma_\mu \nabla \varphi_{(n-1,k)} \gamma_\nu \nabla\, \varphi_{(n+1,k)} \tag{4.8.9}$$

where

$$\varphi_{(n-1,k)} = sinc((n-1)k_1 x) e^{i(n-1)k_1 x} \tag{4.8.10}$$

$$\varphi_{(n+1,k)} = sinc((n+1)k_1 x) e^{i(n+1)k_1 x} \tag{4.8.11}$$

$$\frac{3k_1^2}{(2\pi)^2} = \Lambda \tag{4.8.12}$$

For large values of *n* the Bloch functions statisfy the condition

$$\varphi_{(n-1,k)} \approx \varphi_{(n,k)} \approx \varphi_{(n+1,k)} \tag{4.8.13}$$

The quantum vacuum can therefore be interpreted as a system in which there is a constant annihilation and creation of quanta as implied by Eqn.(4.8.10) and Eqn.(4.8.11) which causes the Nexus graviton to either expand or contract.

4.9 The Hamiltonian formulation in the presence of matter fields

We now seek to introduce matter fields into the quantum vacuum. If we compare the quantized metric of Eqn.(4.2.8) with the Schwarzschild metric we notice that

$$\frac{2}{n^2} = \frac{2GM(r)}{c^2 r} \tag{4.9.1}$$

This yields a relationship between the quantum state of space-time and the amount of baryonic matter embedded within it as follows

$$n^2 = \frac{c^2 r}{GM} = \frac{c^2}{v^2} \tag{4.9.2}$$

Eqn(4.9.2) reveals a family of concentric stable circular orbits $r_n = \frac{n^2 GM}{c^2}$ with corresponding orbital speeds of $v_n = c/n$. Thus in the Nexus Paradigm, unlike in GR, the innermost stable circular orbit ocurrs at $n = 1$or at half the Schwarzchild radius which implies that the event horizon predicted by the Nexus Paradigm is half the size predicted in GR. Also Eqn.(4.9.1) reveals how the Nexus graviton in the *n*-th quantum state imitates DM if *M* is considered as the apparent mass of the DM. Through this comparision, we can also deduce that the deflection of light through gravitational lensing by spacetime in the *n*-th quantum state is

$$\alpha = 4/n^2 \tag{4.9.3}$$

Thus gravitational lensing can be used to constrain the value of the quantum state *n* of space-time within a lensing system.

The result of Eqn.(4.9.2) are added to Eqn.(4.8.9) to yield the time evolution of the quantum vacuum in the presence of baryonic matter as

$$\partial_t(\gamma_\mu \varphi_{(n-1,k)} \gamma_\nu \varphi_{(n+1,k)}) \quad = \frac{1}{4\pi^2} \gamma_\mu \nabla \varphi_{(n-1,k)} \gamma_\nu \nabla\, \varphi_{(n+1,k)} - n^2 \Lambda \gamma_\mu \varphi_{(n,k)} \gamma_\nu \varphi_{(n,k)} \tag{4.9.4}$$

Thus the time evolution of the quantum vacuum in presence of matter resembles thermal flow in the presence of a heat sink. The second term of Eqn.(4.9.4) is an 8-cell or 4-cube that operates as a sinc filter with a four-wave cut-off of

$$k_c^\mu = n k_1^\mu = 2\pi \sqrt{\frac{\Lambda}{3} \cdot \frac{c^2 r}{GM(r)}} \tag{4.9.5}$$

The filtration of high frequencies from the vacuum lowers the quantum vacuum state and generates a gravitational field in much the same way as the Casimir Effect is generated.

Chapter 5

5. The Tully–Fisher relation

In this chapter we derive the Tully –Fisher relation from the new law of gravity Eqn (4.5.9) and show how it evolves with cosmic time.

The Tully-Fisher (TF) relation (McGaugh SS 2011), is an empirical relation between the global HI profile of a galaxy and its (visual) absolute magnitude, which was first been used by Tully and Fisher to determine the distance to the Virgo and Ursa Major clusters. The TF relation constitutes a relation between the dynamical mass and the luminosity (L), which in the case of a constant mass-to-light ratio relate dynamical mass to observed (stellar) mass. This relationship is usually written in the form

$$M(\eta) = A - b\,\eta \qquad (5.1.1)$$

where the absolute magnitude M = const. $-2.5\log(L)$ and $\eta = \log(W) - 2.51$, $W = 2v_{\rm rot}$.

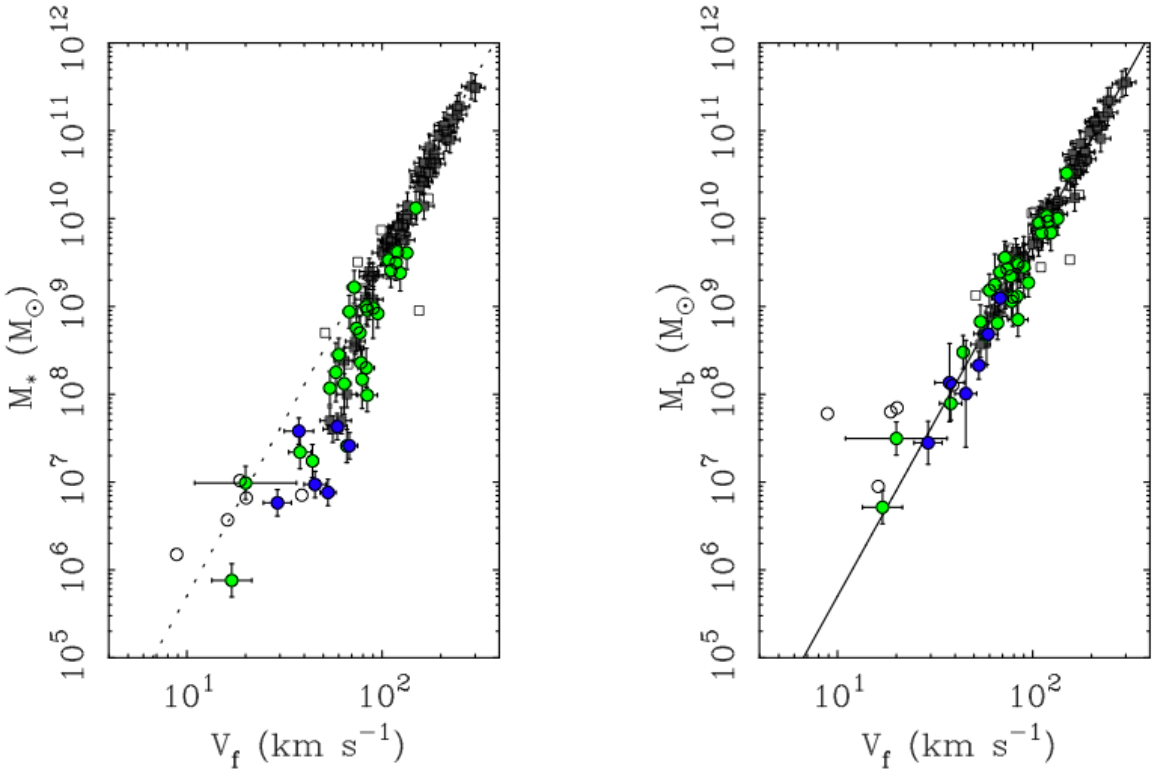

Figure 1: The Tully – Fisher Relation

The Tully-Fisher relation for luminosity against maximum radial velocity

The Tully-Fisher relation for baryonic mass against maximum radial velocity provides a tighter correlation

It was first observed McGaugh and others (McGaugh *et al* 2000,) that baryonic mass was a more fundamental quantity in the Tully-Fisher relation. They highlighted that the physics of galactic kinematics should consider all baryonic mass equivalent. This insight results in a Baryonic Tully-Fisher Relation (BTFR) that is linear (in log space) over many decades in mass. The BTFR then becomes the fundamental physical relation underpinning the empirically observed Tully-Fisher relation. This suggests that the true form of the BTFR is of obvious importance.

Interestingly, a physical theory that can provide a cogent explanation of how the TF relation arises is remains elusive. The tentative classical textbook derivation (e.g. Carroll & Ostlie, 1996) goes as follows:

If a galaxy is considered as a spherically symmetric mass distribution at centrifugal equilibrium then it follows:

$$\frac{v^2}{r} = \frac{GM(r)}{r^2} \qquad (5.1.2)$$

where $M(r)$ is the mass within radius r and v_{rot} is the rotation velocity at this radius. Hence, $v_{rot}^2 \propto \frac{M(r)}{r^2}$. Secondly, assuming that galaxies have a universal mass-to-light ratio M/L and a constant mean surface brightness Σ_0 then

$$\mathrm{L} \propto \Sigma_0 r^2 \tag{5.1.3}$$

hence,

$$v_{rot}^2 \propto \frac{L}{r^2} \propto \frac{L}{\sqrt{\mathrm{L}/\Sigma_0}} \tag{5.1.4}$$

As the object as a whole moves away from the observer one half moves away faster than the other due to rotation. This results in the broadening of the global HI spectrum along the semi major-axis which can be used to estimate the rotation velocity which reduces to:

$$L \propto v^4 \tag{5.1.5}$$

This above result is in agreement with the infrared TF relation and therefore it is thought that this is the most fundamental form. Although this result produces the correct slope, not all the physics is understood. Zwaan et al. (Zwaan et al 1995) showed that the TF relation is not only valid for the standard high surface brightness (HSB) spiral galaxies, but also for low surface brightness galaxies (LSB). This would imply the $M=L$ for LSBs to be different from HSB galaxies. Thus rewriting Eqn. (5.1.4) as:

$$L \propto \frac{V^4}{\Sigma_0 (M/L)^2} \tag{5.1.6}$$

The observation that LSBs must lie on the same TF relation means that also for these galaxies the factor $\Sigma_0 (M/L)^2$ must be constant. Yet, since these galaxies possess a smaller Σ_0 it follows that their mass-to-light ratio must be larger and therefore they must have lower mass-surface densities. Hence, one has to conclude that from a dark matter point of view, the kinematics of these galaxies are dominated by dark matter to a higher degree than HSB galaxies, which makes the existence of the TF relation difficult to understand, since it covers a broad range of luminosities. This problem becomes apparent from the derivation of the equations: Since in general, spiral galaxies have constant rotation velocities out to many times the effective (optical) radii and on the other hand, half of the light originates from one effective radius, it seems problematic to use the same radius in the equation of centrifugal equilibrium (Eqn. (5.1.2)) as in the equation describing the luminosity (Eqn. (5.1.3)).

The underlying problem of understanding the TF is to understand the "disk-halo

conspiracy" (van Albada *et al*., 1985), that is, to find a mechanism that can explain the coupling between dark and luminous matter that distributes them in such a way that at rotation curves result.

In the Nexus Paradigm a much more straight forward derivation is possible from Eqn.(1.1)

$$\frac{d^2r}{dt^2} = \frac{GM(r)}{r^2} + H_0 v_n - H_0 c$$

The first term on the right is the Newtonian gravitational acceleration, the second term is a radial acceleration induced by space-time in the *n*-th quantum state and the final term is acceleration due to DE. The dynamics becomes strongly non-Newtonian when

$$\frac{GM(r)}{r^2} = H_0 c = \frac{v_n^2}{r} \tag{5.1.7}$$

These are conditions in which the space-time curvature due to baryonic matter is annulled by that due to the presence of DE. Under such conditions

$$r = \frac{v_n^2}{H_0 c} \tag{5.1.8}$$

Substituting for *r* in Eqn.(5.1.7) yields

$$v_n^4 = GM(r)H_0 c \tag{5.1.9}$$

This is the Baryonic Tully – Fisher relation. The conditions permitting the DE to cancel out the curvature due to baryonic matter leave quantum gravity as the unique source of curvature. Thus condition (5.1.7) reduces Eqn.(1.1) to

$$\frac{d^2r}{dt^2} = \frac{dv_n}{dt} = H_0 v_n \tag{5.1.10}$$

From which we obtain the following equations of galactic and cosmic evolution

$$r_n = \frac{1}{H_0} e^{(H_0 t)} (GM(r)H_0 c)^{\frac{1}{4}} \quad = \frac{v_n}{H_0} \tag{5.1.11}$$

$$v_n = e^{(H_0 t)} (GM(r)H_0 c)^{\frac{1}{4}} \quad = H_0 r_n \tag{5.1.12}$$

$$a_n = H_0 e^{(H_0 t)} (GM(r)H_0 c)^{\frac{1}{4}} \quad = H_0 v_n \tag{5.1.13}$$

Here r_n is the radius of curvature of space-time in the *n*-th quantum state (which is also the radius of the *n*-th state Nexus graviton), v_n the radial velocity of objects embedded in that space-time, and a_n, their radial acceleration within it. The amplification of the radius of curvature with time explains the existence of ultra-diffuse galaxies and the spiral shapes of most galaxies (Marongwe S 2015). The increase in radial velocity with time explains why early type galaxies composed of population II stars are fast rotators. Eqn.(5.1.13) explains late time cosmic acceleration which began once condition (5.1.7) was satisfied or

equivalently from Eqn. (4.1.16) when the density of baryonic matter was at the same value as that of DE. Thus condition (5.1.7) also explains the Coincidence Problem. At galactic scales, it describes the expansion/growth rate of a galaxy.

5.1 The evolving Baroynic Tully –Fisher Relation

The Nexus paradigm derives the bTFR as a function that evolves with the time (Eqn.(5.1.12)) starting from the time since the galaxy became a system in dynamic equilibrium. The increase in radial velocity with time explains why early type galaxies composed of population II stars, lenticulars in particular, are fast rotators compared younger spiral galaxies of the same mass as illustrated in Figure:2

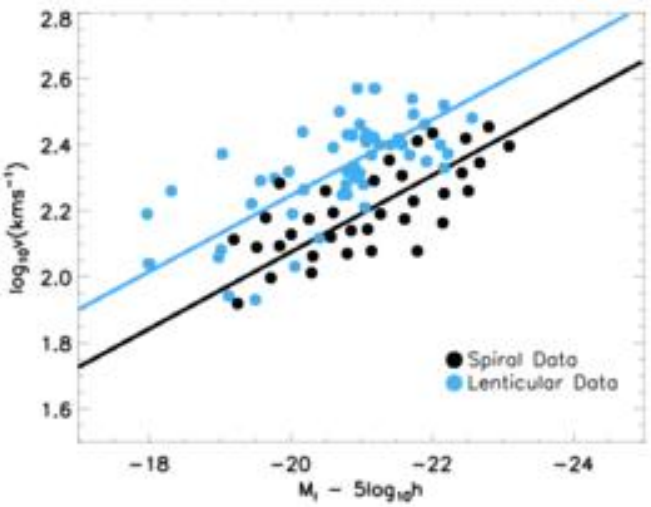

Figure 2: The Tully-Fisher Relation for spiral and lenticular galaxies

The evolving bTFR also provides an explanation of the outlying galaxies observed on a bTFR scatter plot depicted in Fig. 2 and Fig 3. In Fig.3 the relation is depicted from the following equation

$$-logM_b = -4logV_c + \log(GH_0c) + 4H_0(t - t_e)loge \qquad (5.1.1)$$

Here t_e is the age of the red line galaxies measured from the time they acquired dynamic equilibrium. The above relation explains why galaxies of the same baryonic mass may have different rotational speeds and why satellite galaxy clusters have high orbital speeds despite the low baryonic mass content of the main cluster.

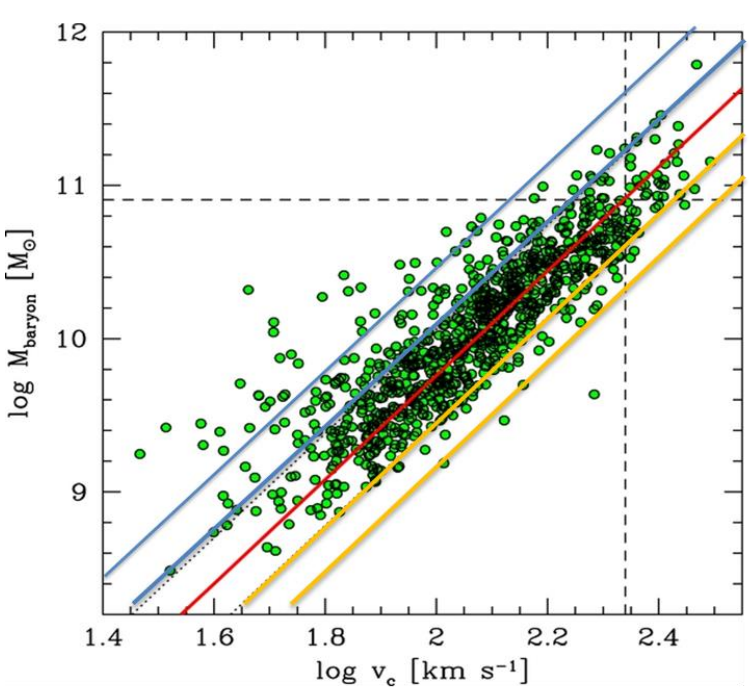

Figure 3: The evolving baryonic Tully-Fisher relation

The evolving bTFR , derived from the Nexus Paradigm, is therefore in agreement with astrophysical observations.

Chapter 6

6.Galaxy rotation curves in the Nexus Paradigm

In this section, galaxy rotation curves predicted by the Nexus Paradigm are compared to observations.

6.1 The galaxy rotation curve problem

The observed kinematics of stars and gas in galaxies do not obey Keplerian dynamics as in the solar system. The standard Newtonian laws of dynamics relating gravity to the observed distribution of observable matter cannot explain the stellar dynamics. This phenomenon is known as the galaxy rotation curve problem and was first observed by Vera Rubin and Kent Ford (Rubin VC & Ford KW 1970). The galaxy rotation curve data show empirical evidence of a tight correlation between the observed mass distribution and the corresponding galactic dynamics. Three empirical rules sum up the properties of rotationally supported galaxies:

1.Rotation curves approach an approximately constant velocity that persists indefinitely (flat rotation curve)

2. The observed mass scales as the fourth power of the amplitude of the flat rotation (the Baryonic Tully-Fisher Relation).

3. There is a one-to-one correspondence between the radial force and the observed distribution of baryonic matter (the mass discrepancy–acceleration relation) .

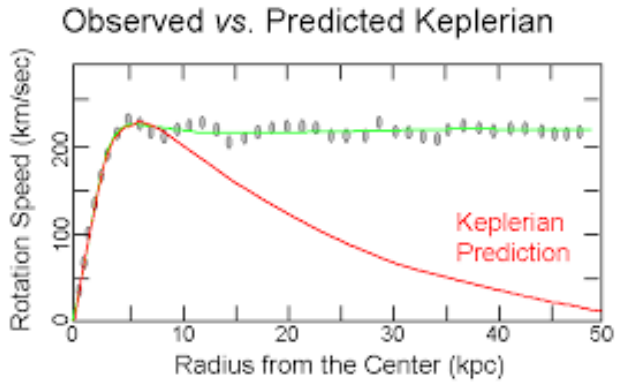

Figure 4: The galaxy rotation curve problem

Fig. 4 shows a rotation curves that depicts the behaviour of disk galaxies. Observations show that, the rotation curves become approximately flat at large radii. This contrasts with the expected Keplerian curve from the enclosed mass of stars and gas. This provides one of the clearest examples of the mass discrepancy.

6.2 The simulation of galaxy rotation curves

In this section, the observational data of the rotation curve of a galaxy is intepreted by computing the orbital speeds as a function of the distance from the galactic centre. The speeds depend on all the mass enclosed within a sphere of that radius. Since a spiral galaxy is composed of a central spherical bulge, a disk of gas and stars, a spherical halo of stars. The contributions from each component are summed up.

$$M = M_{stars} + M_{HI} + M_{DB} \tag{6.2.1}$$

6.3 The equations of galactic kinematics

For ease of calculations, a galaxy is considered such that the density of visible matter, ρ(r), contains an inner core at radius r = r_c. The acceleration law of equation (1.1) takes the form

$$\frac{v^2}{r} = \frac{GM(r)}{r^2} + H_0 v - H_0 c \tag{6.3.1}$$

From which we find

$$v = \frac{1}{2}H_0 r + \frac{\sqrt{{H_0}^2 r^2 + 4r\left(\frac{GM(r)}{r^2} - H_0 c\right)}}{2} \tag{6.3.2}$$

This law reduces to Eqn (5.12) $v_n = e^{(H_0 t)}(GM(r)H_0 c)^{\frac{1}{4}} = H_0 r$ once condition (5.1.7) has been satisfied.

The total mass M(r) of a sphere of radius r is given by the expression

$$M(r) = 4\pi \int_0^r r^2 \, \rho(r) dr \tag{6.3.3}$$

A simple model of M(r) is

$$M(r) = M_0 \left(\frac{r}{r_c + r}\right)^{3\beta} \tag{6.3.4}$$

Where β= 1 for HSB galaxies and β= 2 for LSB galaxies

Well inside the core radius, the density is constant for HSB galaxies. However, for LSB galaxies the density follows the trend $\rho(r) \propto (r/r_c)^3$. The high resolution rotation curves for the LSB galaxies provide a clean testing ground for any theory of galaxy rotation curves.

6.4 The computational method for the rotational curves

The exponential term in the equation $v = e^{(H_0 t)}(GM(r)H_0 c)^{\frac{1}{4}}$ is considered to approximate unity for a galactic system that is less than 4 billion years old since it attained dynamic equilibrium. The equation is then reduced to

$$v = (GM(r)H_0 c)^{\frac{1}{4}} \tag{6.4.1}$$

If we know the asymptotic velocity v_c from the data then Eqn. (6.4.1)for LSB galaxies is reduced to

$$v = (GM_0 H_0 c)^{\frac{1}{4}}(\left(\frac{r}{r + r_c}\right)^6)^{\frac{1}{4}}$$

$$v = v_c(\left(\frac{r}{r+r_c}\right)^6)^{\frac{1}{4}} \tag{6.4.2}$$

Next we input the radius data from (Kuzio de Naray *et al*.2006 & Kuzio de Naray *et al*.2008) and r_c is adjusted to give the best line of fit. Adjusting r_c is adjusting the average baryonic density of the galaxy. A large r_c implies a low average baryonic mass density while a low r_c implies a high average density.

The following are the respective constants in SI units:

Gravitational constant G = 6.67259 x 10^{-11} m^3 kg^{-1} s^{-2}

1 solar mass = 1.989 x10^{30} kg, 1 kilo parsec = 3.086 x10^{19} m Hubble constant=2.2 x 10^{-18} s^{-1}

In Fig. 5 the predicted and observed rotation curves of six LSB galaxies are displayed. For the predicted curve (red line), the average baryonic density of each galaxy is kept constant by keeping the value of r_c in Eqn.(6.4.2) constant.

6.5 Results

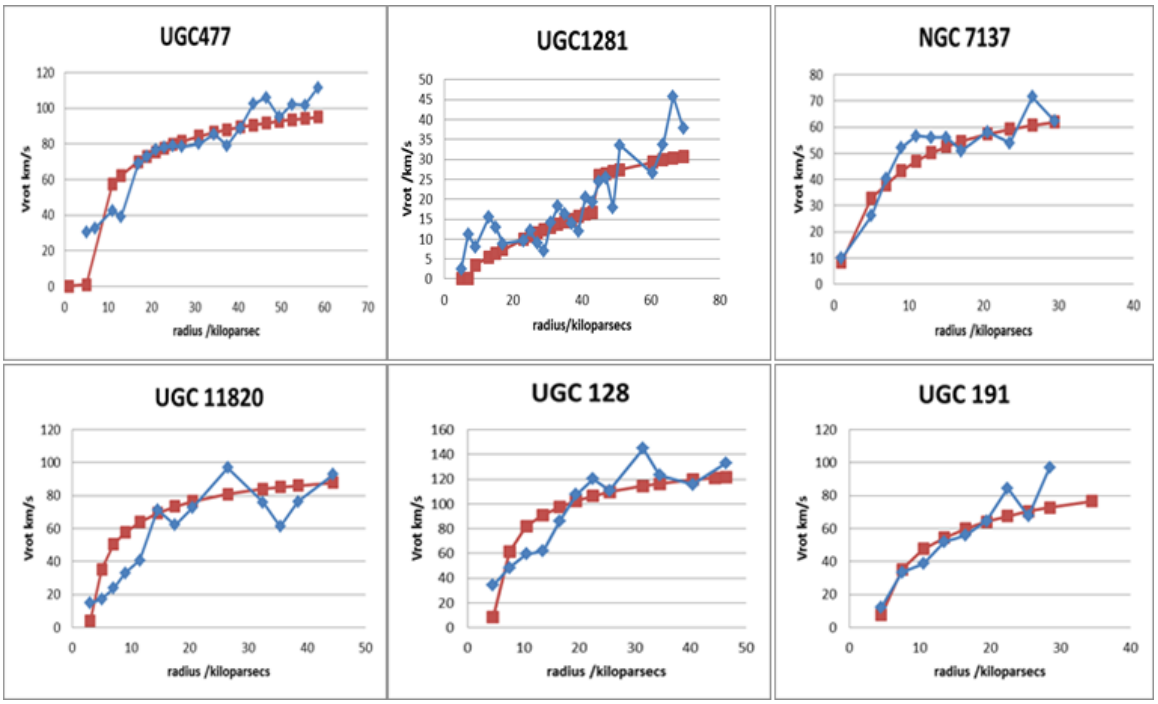

Figure 5: galaxy rotation curves for LSB galaxies

The blue curve is the observed data and red is the curve obtained from theory. The average baryonic density of each galaxy is kept constant by keeping the value of r_c in Eqn(6.4.2)constant.

Chapter 7

7.Probing Quantum gravity through aLIGO and VIRGO observations

7.1 Gravitational waves

Gravitational waves were first predicted by Albert Einstein in 1916 and are a result of disturbances in the fabric of space-time caused by violent and energetic processes in the Universe. GR shows that massive accelerating objects such as neutron stars or black holes orbiting each other, disrupt space-time in such a way that gravitational waves would radiate from the source. Gravitational waves offer another means of obtaining information from these cataclysmic events since they carry information about their cataclysmic origins.

Strong gravitational waves are produced by colliding black holes, supernovae, merging neutron stars or white dwarf stars and the slightly wobbly rotation of neutron stars that are not perfect spheres

7.2 The LIGO Scientific Collaboration (LSC)

The LSC is a group of scientists whose aim is to directly detect gravitational waves. Their detection and analysis is then used to explore the fundamental physics of gravity, and to decode the nature of the astrophysical cataclysms that spawned them. Their work is also focused toward development of techniques for, gravitational wave detection; and the development, commissioning and exploitation of gravitational wave detectors.

The LSC executes its mission using LIGO Observatories, located in Hanford, Washington and Livingston, Louisiana as well as that of the GEO600 detector in Hannover, Germany. Their research is centered around the following areas:

- **analysis of LIGO and GEO data**
- **searching for gravitational waves from astrophysical sources**
- **detector operations and characterization**

- **development of future large scale gravitational wave detectors.**

The LSC was founded in 1997 and is currently made up of more than 1000 scientists from over 100 institutions and 18 countries worldwide. .

7.3 The LIGO Observatory

LIGO currently consists of one detector in Hanford Washington and the other in Livingston, Louisiana operated in unison as a single observatory. LIGO is operated by a consortium of the California Institute of Technology (Caltech) and the Massachusetts Institute of Technology (MIT) and is funded by the National Science Foundation.

7.4 Predicted and observed merger speeds

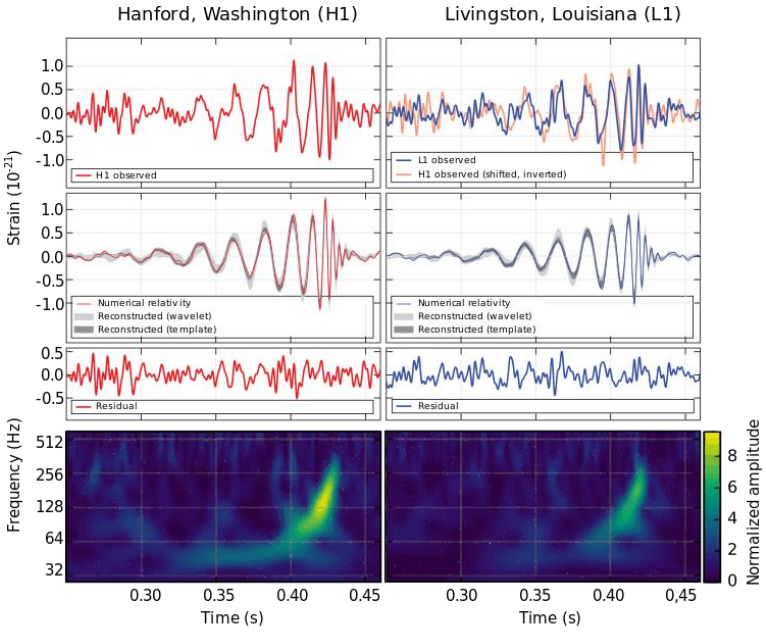

Figure 6: LIGO measurements of GW150914

LIGO measurements of GW150914 by both Livingstone (right) and Hanford detectors (left)

The first detection of gravitational waves by the aLIGO detectors was made on September the 14th 2015. An analysis of the signal along with the inferred redshift suggested that it was produced by the merger of two black holes of approximately 35 and 30 solar masses, resulting in a post-merger black hole of 62 solar masses(Abbot BP et al 2016). This implied that a mass deficit of 3 solar masses was radiated away as gravitational wave energy.

The detected waveform matched that predicted from numerical relativity simulations. However, the maximum relative merger speed predicted by numerical relativity is 0.4 *c* where *c* is the speed of light whereas that which was observed from GW150914 was slightly above 0.5*c*. This tension between theory and observation has consistently manifested in subsequent observations as displayed in Table 1

Table 1

Signal	approx.Binary mass/M* (solar Mass)	Frequency/Hz (approx. at maximum amplitude)	Approx. Speed/*c*
GW150914	65^{+5}_{-4}	150	0.53
GW151225	$22^{+6.1}_{-1.7}$	450	0.54
GW170104	50.7^{+7}_{-6}	200	0.54
GW170814	55^{+4}_{-4}	200	0.55
GW190521	151.0^{+21}_{-16}	60	0.52
GW190412	$38.4^{+3.8}_{-3.9}$	211	0.50

The speed is obtained by inputting the observed data into the post-Newtonian parameter

$$\frac{v}{c} = \left(\frac{GM\pi f}{c^3}\right)^{\frac{1}{3}} \qquad (7.5.1)$$

In the Nexus paradigm, the spacetime in close proximity to a black hole is in the $n = 2$ quantum state since the $n = 1$ state is within the black hole. The importance of this state lies in that it allows GW telescopes to detect quantum gravity effects. Time dependent perturbations of this state will result in an additional potential $V(t)$to the unperturbed state. Eqn. (4.9.2) can be written as

$$v^2 = \frac{c^2}{n^2} = \frac{GM(r)}{r} \qquad (7.5.2)$$

Taking into consideration of the time dependent perturbation, Eqn.(8.5.2) becomes

$$v^2 = \frac{c^2}{n^2} + V(t) \; = \frac{GM(r)}{r} + V(t) \qquad (7.5.3)$$

This implies that the speed of an inspiraling black hole before merging (in the n = 2 state) is always slightly above $c/2$ which is in agreement with observations thus far. The perturbing potential $V(t)$ can be calculated using strong perturbation theory.

Chapter 8

7. Probing Quantum Gravity with the Event horizon Telescope

The Event Horizon Telescope (EHT) is an international collaboration aimed at studying the extreme gravity regime near the event horizon of a black hole. Their key science objectives are:

- **Imaging a black hole:** The EHT collects submillimeter radio waves from the black hole event horizon using Very Large Baseline Interferometry (VLBI). The VLBI consists of currently eight telescopes distributed around the Earth. Once the EHT has measured data from the black hole, image processing begins which takes many months to complete using super computers because of the huge amount of collected data.
- **Testing General Relativity using the black hole shadow:** GR is currently the best theory of gravity and is still yet to be tested in extreme gravity environment of the event horizon. Due to the phenomenon of gravitational lensing GR predicts a shadow of specific size and shape for a given black hole. The EHT aims to detect any deviations from this prediction
- **Understanding accretion around a black hole:** The formation of an accretion disc around a black hole still remains a mystery . By observing the event horizon the EHT collaboration aims to understand the formation mechanism involved.
- **Understanding jet genesis and collimation:** The mechanism for the formation of black hole jets and their collimated structure is one of the deepest mysteries in black hole physics. It is hoped that observations of the event horizon of M87 will shed light on the mechanism.

The EHT presents an opportunity to test alternative theories of gravitation and in this case the Nexus Paradigm of quantum gravity. The theory predicts a circular shadow which is half the size predicted in GR. Moreover, this shadow is embedded within a disc of four times the shadow diameter- a feature which further distinguishes it from GR. Fig. 7 shows the predicted shape and size of Sagittarius A* (Sgr A*), the black hole at the center of the Milky Way galaxy under observation by the EHT . The EHT has been observing Sgr A*

since 2008 (Doeleman S *et al* 2009, DoelemanS et al 2016) and has been improving the image resolution over the years.

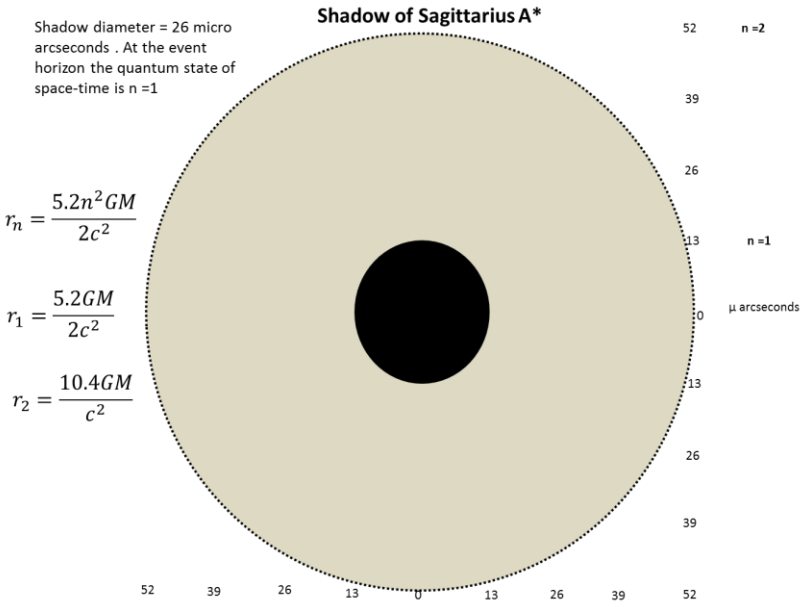

Figure 7: Shadow of Sagittarius A*

The latest image at a resolution of 30 microarcseconds from (Lu RS *et al* 2018) is depicted in Fig.8. The results thus far indicate that the shadow is half that predicted by GR (white circle) and indeed lies inside a disc of four times the shadow diameter. The final image will be released in the second or third quarter of 2020.

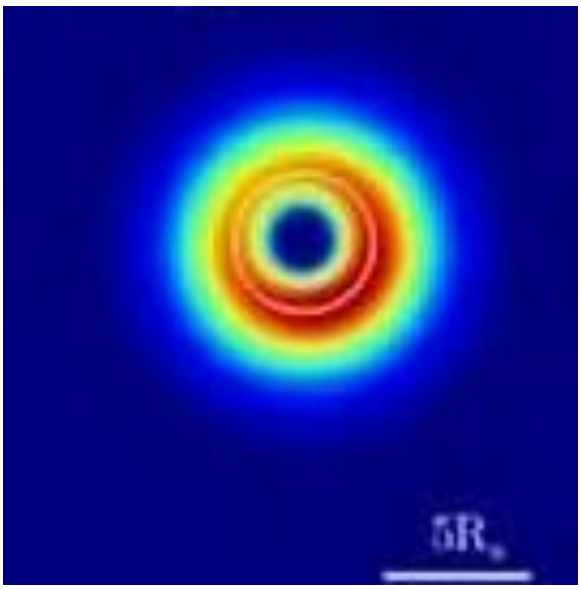

Figure 8: Image of Sagittarius A* from the 2013 EHT campaign showing a central dark spot of 26 microarcseconds in diameter and a base diameter of approximately 104 microarcseconds.

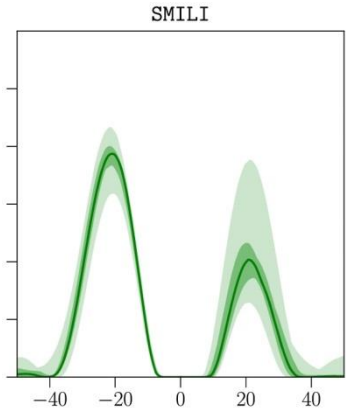

Fig 9.
Image cross section of M87* showing a central dark spot of approximately 20 microarcseconds in diameter and a base diameter of approximately 80 microarcseconds. Image courtesy EHT Collaboration

The image of M87* released by the Event Horizon Telescope Collaboration in 2019 (Fig.9) shows a dark spot of diameter half the size of a shadow predicted by GR surrounded by a thick emission ring constituting a large portion of a penumbra four times the size of the dark spot.

Conclusions

The astrophysical observations that were presented show that the Nexus Paradigm is a viable alternative theory of gravity . On Galactic kinematics, the Nexus Paradigm derives the baryonic Tully –Fisher relation from first principles. This is a critical requirement of any theory that attempts to explain galactic kinematics. Moreover, the Nexus Paradigm delves further in demonstrating that the baryonic Tully-Fisher relation evolves over cosmic time and therefore providing an explanation for the high rotational speed of early type galaxies and population II stars. This work has also provided a method of computing galaxy rotation curves from the Nexus Paradigm which are in good agreement with observations. These features are absent in GR in its original form and still struggles to explain galactic dynamics even with the *ad hoc* inclusion of hypothetical DM.

The aLIGO observations give tantalizing evidence that black hole mergers occur at relative speeds slightly above half the speed of light in agreement with the Nexus Paradigm whereas numerical relativity predicts a maximum speed of 40% the speed of light which is in tension with observations.

Finally the latest observations by the EHT show a shadow with the predicted shape and size from the Nexus Paradigm. The size predicted by GR is at tension with observations.

In synthesis, the Nexus Paradigm is a viable falsifiable candidate for a quantum theory of gravity from which new physics could be discovered if more attention is given to it by the physics community.

References

Aalseth C et al 2011 *Phys. Rev. Lett.* **106**(13) 131301.

Abbot B P et al 2016 arxiv:1602.03837

Ade P A R *et al* 2013 *a* arXiv: 1303.5062

Ade P A R *et al* 2013 *b* arXiv: 1303.5076

Akerib D S *et al* (LUX Collaboration) 2017 *Phys.Rev.Lett*. **118** 021303

Ambjorn J 2013 arxiv:1302.2173 [heo-th]

Anderson E 2004 arxiv: gr-qc/0409123v1

Anderson E 2010 arxiv:1009.2157 [gr-qc]

Archambault S *et al*. 2009 [PICASS0 Collaboration] *Phys. Lett. B* **682**(2) 185–192.

Ashtekar A 1986 Phys. Rev. Lett.57:2244

Atiyah M *et al* 2017 arxiv:1704.07464v2 [hep-th]

Baker C *et al* 1999 *Mon. Not. R. Astron. Soc.* **308**(4) 1173–1178.

Bekenstein J D 2006 *Contemp. Phys.* **47** 387.

Boller T H 1989 *Astron. Nachr* **310**,362

Bullock J S & Boylan-Kolchin 2017 *Annual Review of Astronomy and Astrophysics* 55 343-387

Capozziello S 2002 *Int. J. Mod. Phys. D* **11** 483–491

Capozziello S *et al* 2013 *Galaxies 2013* **1** 216–260.

Carroll BW & Ostlie DA 1996 Cummings 1996 ISBN 0-201-54730-900/1996

Chiba T *et al* 2007 *Phys. Rev. D* **75** 124014.

Clowe D *et al* 2006 *Astrophys.J.* **648**(2) (2006) 109–113.

Clowe D *et al*, 2012 *Astrophys.J.* **758**,128

Cui X *et al* 2017 arxiv:1708.06917v2 [astro-ph.CO]

Cushman P *et al* 2013, *Preprint* hep-ex.1310.8327v2

Dent J B 2011 *J. Cosmol. Astropart. Phys.* **2011** (2011) 009.

De Blok WJG 2009 *preprint [astro-ph.CO]* 0910.3538v1

Deser S 2017 arxiv:1706.02448[physics.hist-ph]

DeWitt B S 1967 . *Phys.Rev*. 160 (5): 1113–1148

Doeleman S *et al* 2009 arxiv:0906.3899 [astro-ph.CO]

Doeleman S *et al* 2016 arXiv:1512.03818 [astro-ph.CO]

Eichhorn A 2017 arxiv:1709.03696[gr-qc]

Ellis R S 2010 *Phil. Trans. R. Soc. A* 2010 **368** 967-987

The Event Horizon Telescope Collaboration (2019) Astrophysical Journal Letters, 875:L4

Faber S M *et al* 1976 *Astrophys. J.* **204** (1976) 668–683.

Famaey B and McGaugh S S 2012 *Living Rev. Relativ.* **15** (2012) 10.

Federico L, McGaugh S and Schombert J M 2015 *Preprint[astrp-ph.GA]* 1512.04543v1

Ferrero I, Abadi M G, Navarro F J, Sales and V J, Gurovich S 2012 *MNRAS*, **425** 2817-2823

Finister F 2016 arxiv:1605.04742v2 [math-ph]

Friedel L 2005 arxiv: hep-th/0505016

Gambini R and Pullin J 1996 Cambridge University Press 1996

Gibbons GW and Hawking SW 1993 World Scientific Publishing ISBN-13978-9810205157

Goodman M and Witten E 1985 *Phys.Rev. D* **31**(2) 3059.

Green B, Schwarz J H,and Witten E 1987 Cambridge UK, Univ. Pr. 596p

Herczeg G 2017 arxiv:1709.08825[gr-qc]

Immirzi G 1997 arxiv-gr-qc/9701052v1

Israel M *et.al*, 2014 *A&A* **564**,129

Jauzac M *et al* 2015 *MNRAS* **446**,4132-4147

Jee M J, Mahdavi A, Hoekstra H, Babul A, Dalcanton J J, Carroll P, and Capak P 2012 *The Astrophysical Journa*l **747** (96)

Jee M J, Mahdavi A, Hoekstra H and Babul A 2014 *The Astrophysical Journa*l **783** (78)

Kiefer C and Kramer M 2012 *Int. J. Mod. Phys. D* **21** (2012) 1241001

Kiefer C 2013 *Math.Phys.* **2013** 509316

Kiritsis 1998 Leuven Univ. Pr 315p [hep-th/9709062]

Kitching T *et al*, 2015 *Astronomy and Computing* **10** 9-21

Komatsu E *et al* 2009 *Astrophys. J. Suppl.* **180**(2) 330–376.

Kuzio de Naray *et al*. 2006, ApJS, **165**, 461

Kuzio de Naray *et al*. 2008, ApJ, **676**, 920

Leauthaud A *et al* 2015 *MNRAS* **446** 1874-1888

Lee J, and Komatsu E 2010 *Astrophysical Journal* **718** 60-65

Li B, Sotiriou T P and Barrow J D 2011 *Phys. Rev. D* **83** 104017.

Lisi AG 2007arxiv:0711..0770v1 [hep-th]

LUX Collaboration 2013 arXiv: 1310.8214v2 [astr0-ph.CO].

Lu RS *et al* 2018 *ApJ* **859** 60

Malament DB 2000 arxiv:gr-qc/0011094

Marongwe S 2015 *Int. J. Geom. Methods Mod. Phys.* **12**(4) 1550042,

Marongwe S 2017 *Int. J. Mod. Phys. D* **26** 1750020

Massey R *et al* , 2013 *MNRAS* **429**, 661-678

McGaugh S S *et al* 2000 arxiv: astro-ph/0003001

McGaugh S S 2005 *The Astrophysical Journal* **632** (2)

McGaugh S 2011*Preprint [astro-ph]* 1107.2934v2

McGaugh 2014 S *Canadian Journal of Astrophysics* **93**(2) 250-259

Milgrom M 1983 *Astrophys. J.* **270** 371–389.

Milgrom M and McGaugh S S 2013 , *Astrophys. J.* **766**(1) 22.

Minchin R *et al* 2005 *Astrophys. J. Lett.* **622** L21–L24.

Navarro J , Carlos F S and Eke V R 1996 *MNRAS.* **283**(3) L72-L78

Nottale L 2008 arxiv: 0812.3857v1 [physics.gen-ph]

Olmo G J 2005 *Phys. Rev. D* **72** 083505

Percacci R 2007 arxiv:0709.3581 [hep-th]

Perlmutter S *et al.* 1999 *Astrophys. J.* **517**(2) 565–586.

Reid DD 1999 arxiv:gr-qc/9909075

Riess A *et al*, 1998 *Astron. J.* **116**(3) 1009–1038.

Rovelli C 2011, arxiv:1102.3660 [gr-qc])

Rubin VC & Ford K W 1970 *Astrophys. J* **159**.p.379 R

Sanders R H *et al* 2002 *Ann. Rev. Astron. Astrophys.* **40** 263–317

Sangalard V *et al.* 2005 *Phy. Rev. D* **71**(12) 122002.
Se-Heon O *et al* 2015 *The Astronomical Journal* **149** (6)

Setare *et al* 2013 *Canadian J. Phys.* **91** 260–267.

Smolin L 2005 arxiv: hep-th/0507235

Starobinsky A 1979 *JETP Lett.* **30** 682

Tan A *et al* (Panda X-II Collaboration) 2016 *Phys.Rev.Lett*. **117** 121303

Tegmark M *et al* 2004 *Phys. Rev. D* **69** 103501.

The CDMS II Collaboration 2010 *Science* **327**(5973) 1619–1621.

Thompson R, Dave R and Nagamine K 2014 *Preprint [astro-ph.CO]*1410.7438v2

Van den Bosch F C and Swaters R A 2001 *MNRAS*, **325** (3) 1017-1038

Vikhlinin A *et al* 2006 *Astrophys. J.* **640**(2) 691–709

Volovik GE 2000 arxiv:gr-qc/0005091v3

Wang A 2017 arxiv:1701.06087

Wu P *et al* 2010 *Phys. Lett. B* **693** 415–420.

Zhandov V I, Alexandrov A N, Fedrova EVK and Sliusar V M 2012 *Astronomy and Astrophysics* **2012**, Article ID 906951

Zwicky F 1937 *ApJ86,***217**

Zweibach B 2004 Cambrige UK: Univ. Pr 558p